



BIO 301

END SEMESTER REPORT

Study of host-parasite interaction proteins
in case of Plasmodium falciparum mediated
malaria and in-silico prediction of peptide-
based inhibitors for crucial interactions

AUTHOR

Antony Kiran K David
20181083

BS-MS student, IISER Pune

SUPERVISOR

Dr Sanjeev Galande

Division of Biology, IISER Pune

Sept 2020 – Dec 2020

CONTENTS

Acknowledgements.....	3
List of Tables	4
List of Figures	4
1 Abstract.....	5
2 Introduction.....	5
3 Materials and methods	6
3.1 Obtaining the complex from Protein Data Bank and Pre-processing.....	6
3.2 Identifying the interacting region	6
3.3 Computational Saturated Mutagenesis and scoring	7
3.4 Molecular Dynamics simulation of the inhibitor models and its analysis	7
4 Results and findings.....	8
4.1 Obtaining the complex from Protein Data Bank and Pre-processing.....	8
4.2 Identifying the interacting region	9
4.3 Computational Saturated Mutagenesis and scoring	9
4.4 Molecular Dynamics simulation of the inhibitor models and its analysis	10
4.4.1 Inhibitor 1: Hybrid.....	11
4.4.2 Inhibitor 2: Mutant	13
4.4.3 Inhibitor 3: Mutant	14
4.4.4 Inhibitor 4: Mutant	16
5 Discussion	17
6 Conclusion	18
7 References.....	18

ACKNOWLEDGEMENTS

This work was done as part of the 2020 iGEM project from IISER Pune titled: Anopheles: "The Half Blood Princess" (<https://2020.igem.org/Team:IISER-Pune-India>). The project aimed to develop a peptide-based drug library to combat the problem of Drug resistance among the Plasmodium parasites. The whole Team conceived the idea of the project. It was brought to completion by constant help and support from our mentors.

I would like to thank Dr Madhusudhan M S and Tejashree Kanitkar for helping in planning the bulk of the methods used in this project. I would like to thank the Dry Lab team members, especially Aleena Jose and Anantha S Rao for helping me with writing the scripts required for the analysing the data. I would like to thank Rashim Malhotra for helping me complete this project report.

I would like to thank the PARAM BRAHMA facility under the National Supercomputing Mission, Government of India at IISER Pune for providing the required computational resources for the project.

This project would be incomplete without the help and constant support from our PI Dr Sanjeev Galande. I would like to thank him for being such a fantastic PI to the Team.

I would like to thank IISER Pune, iGEM Foundation, all the sponsors of the iGEM 2020 team for providing me with this opportunity.

Finally, I would like to thank all my team members and mentors for their constant support and criticism during the entire period of the project.

LIST OF TABLES

Table 1: Deleted residue number after homology modelling	8
Table 2: Summary of potential inhibitors	10
Table 3: Summary of MD simulation data. (*: MD simulation was not performed; Centroid distance and hydrogen bond numbers were calculated based on the homology model from SWISS MODEL after identifying the interacting regions).	10
Table 4: Abundance of hydrogen bond pairs of inhibitor 1	12
Table 5: Abundance of hydrogen bond pairs of inhibitor 2	14
Table 6: Abundance of hydrogen bond pairs of inhibitor 3	15
Table 7: Abundance of hydrogen bond pairs of inhibitor 4	17

LIST OF FIGURES

Figure 1: Interaction complex after homology modelling. The CIDRa domain is shown red and CD36 receptor protein in blue.	8
Figure 2: Identified wild type inhibitor. The inhibitor is shown in blue and the parasite protein in red	9
Figure 3: Heat map summarising the result of Computational Saturated Mutagenesis.....	9
Figure 4: RMSD plot of inhibitor 1	11
Figure 5: Centroid plot of inhibitor 1	11
Figure 6: Hydrogen bond plot of inhibitor 1	12
Figure 7: RMSD plot of inhibitor 2	13
Figure 8: Centroid plot of inhibitor 2	13
Figure 9: Hydrogen bond plot of inhibitor 2	14
Figure 10: RMSD plot of inhibitor 3	14
Figure 11: Centroid plot of inhibitor 3	15
Figure 12: Hydrogen bond plot of inhibitor 3	15
Figure 13: RMSD plot of inhibitor 4	16
Figure 14: Centroid plot of inhibitor 4	16
Figure 15: Hydrogen bond plot of inhibitor 4	17

1 ABSTRACT

Malaria is caused by the Plasmodium parasites and is transmitted through the bites of female Anopheles mosquito. Of the 5 Plasmodium species that cause malaria, *P. falciparum* and *P. vivax* cause the greatest threat. The unavoidable problem of drug resistance among the parasites is significantly affecting our battle against this deadly infection. To tackle this problem the 2020 iGEM team from IISER Pune has proposed developing a peptide drug library. So when we observe that the parasite has developed resistance against one drug, we could choose a different one available in the library.

This study is part of that effort where I would be investigating the cytoadherence promoting interaction between Plasmodium falciparum PfEMP1 virulence protein and human host CD36 receptor and predicting a peptide-based inhibitor for the interaction using in-silico analysis.

2 INTRODUCTION

Malaria is a mosquito-borne protozoan disease caused by the Plasmodium parasites. It poses a great threat to public health, especially in developing countries, including India. The most dangerous form of malaria is caused by *P. falciparum* and *P. vivax*, of which *P. falciparum* is more prevalent in India.

In 2019 alone, there is an estimated 229 million infections and 409000 deaths due to malaria. In 2018, *P. falciparum* accounted for 99.7% of estimated malaria cases in the WHO African Region, 50% of cases in the WHO South-East Asia Region. [12]

The fact that makes *P. falciparum* more deadly is that it gets replicated very quickly in the blood; hence building up the infection quickly. So if the person is not diagnosed with 2-3 days, the infection may become severe. [11]

One additional complication in case of falciparum malaria is that, during the stage of 48-hour intraerythrocytic life cycle of *P. falciparum*, it causes many changes to the morphology of RBC [8]. The PfEMP1 proteins protruding from the membrane of the infected RBC causes the sequestration of it to the microvasculature. This helps in preventing splenic clearance and is responsible for the quick build-up of infection. Apart from this, it can lead to the blockage of the blood vessels which carry blood to various organs and deprive it of oxygen. When this happens to the brain, it is called cerebral malaria, which is fatal [9].

Over the last five decades, *P. falciparum* has developed resistance against most of the approved drugs. Latest epidemiological studies have revealed that the prevalence of drug resistance against the first-line drug Artemisinin spreading in Southeast Asia with the first case of Artemisinin resistance being reported in West Bengal, India [6].

In recent times, protein-protein interactions are gaining importance as potential candidates for therapeutic studies [1]. Studying these protein-protein interactions will help us in gaining

insights into the pathology of the diseases and help in designing peptide-based drugs against it.

To tackle the problem of drug resistance in *P. falciparum*, the 2020 iGEM team of IISER Pune is designing a peptide-based drug library against various host-parasite protein interactions of falciparum malaria. These inhibitors, which are approximately 10 amino acid long, can then be grafted to cyclotide backbone. Cyclotides are now emerging a preferred drug scaffold due to stability which helps in easy transportation and opens up a possibility for oral drug administration [5]. This study is a part of our project where I would be investigating the cytoadherence promoting interaction between Plasmodium falciparum PfEMP1 virulence protein and human host CD36 receptor and predicting a peptide-based inhibitor for the interaction using in-silico analysis. PfEMP1 is a class of membrane proteins expressed on the *P. falciparum*-infected erythrocyte membranes, and CD36 is a scavenger receptor involved in fatty acid metabolism, innate immunity and angiogenesis. It helps in the uptake of long-chain fatty acids. Approximately 84% of PfEMP1 proteins contain domains predicted to bind to CD36, making this the most common adhesion phenotype and an excellent interaction to design peptide inhibitors against [8].

The study involves obtaining the interaction complexes from the Protein Data Bank [2], which is followed by a pre-processing step before identifying the region of the CD36 receptor that interact with the PfEMP1 receptor. This was followed by a round of computational saturated mutagenesis on the identified region. The mutants obtained were shortlisted based on the interaction energies. The shortlisted mutant and wild type interactions were studied further by performing Molecular Dynamics simulations.

We also tried to study the stability of the grafted cyclotide by performing MD simulations.

3 MATERIALS AND METHODS

3.1 OBTAINING THE COMPLEX FROM PROTEIN DATA BANK AND PRE-PROCESSING

The interaction complex of CD36 receptor and CIDRa domain of PfEMP1 was available on Protein Data Bank with PDB ID: 5LGD. The 5LGD PDB contains two chains: chain A which represents the CD36 receptor and chain B which represents the CIDRa domain of the PfEMP1 protein. Apart from these, the complex also contained a small oligosaccharide and few small molecules. To account for the missing regions in the complex, homology modelling was done on the SWISS MODEL homology modelling server using the same PDB ID as the template [18].

3.2 IDENTIFYING THE INTERACTING REGION

As the strategy used to inhibit the interaction was to design a competitive peptide inhibitor, motifs were identified on the CD36 receptor (chain A) which interacted with the PfEMP1 protein (chain B) using knowledge-based approaches. All the amino acid sequences that fall within a particular threshold were treated as potential wild type inhibitors.

3.3 COMPUTATIONAL SATURATED MUTAGENESIS AND SCORING

Saturated mutagenesis is a protein-engineering technique in which amino acid at each position is substituted with all possible amino acids to yield mutants. This is used for improving specific characteristics of proteins like catalytic activity, thermostability and binding affinity, among others [14].

A custom python script built on top of UCSF Chimera [16] was used to perform computational saturated mutagenesis on the identified wild type inhibitor.

The mutants were scored based on the interaction energy values obtained by FoldX [17]. The AnalyseComplex function of FoldX was used for this. All the mutants were first optimised using the RepairPDB function of FoldX before calculating the interaction energy.

Based on the interaction energy values, a hybrid inhibitor was also constructed with the best scoring (most negative interaction energy) amino acid at each position.

3.4 MOLECULAR DYNAMICS SIMULATION OF THE INHIBITOR MODELS AND ITS ANALYSIS

Molecular Dynamics (MD) simulations were performed in triplicates for the 3 best mutants and also the hybrid to study its stability in a simulated system using GROMACS 2019.1.

The topology file was generated using the AMBER99SB-ILDN force fields [10] and solvated it using the SPC/E water model [13]. A water box of a minimum solute-box distance of 1 nm was used to solvate each system. Sodium and chloride ions were added to achieve charge neutrality by replacing the required number of solvent molecules. The Particle mesh Ewald (PME) sum method [4] was used to treat the electrostatic interactions and LINCS algorithm [7] to constrain the hydrogen bond length.

A time step of 2 fs was used for the integration. The whole system was minimised for 50000 steps or till the maximum force was less than $1000 \text{ kJ mol}^{-1} \text{ nm}^{-1}$. The system was then heated to 300 K in an NVT ensemble simulation of 100 ps using Velocity Rescaling thermostat [3]. The pressure was stabilised in an NPT ensemble for 100 ps using Parrinello-Rahman barostat [15]. The optimised system was then simulated for 100 ns, where the temperature and pressure were regulated by the Velocity rescaling thermostat [3] and Parrinello-Rahman barostat [15] respectively. The snapshots of the structure were taken at every 500ps, starting from zero. The temperature and potential energy of the system were monitored for anomalies.

All MD simulations were performed on the PARAM BRAHMA facility under the National Supercomputing Mission, Government of India at IISER Pune.

We visualised the trajectory files to see how the inhibitor interacted with the parasite protein. Periodicity in the system was accounted for by applying coordinate correction using the trjconv utility in GROMACS with the nojump parameter. Root Mean Square Deviation (RMSD) plots with respect to the backbone were calculated using the rms utility in GROMACS to verify

the stability of the complex. The time evolution of distance between the centroids of the inhibitor and the PfEMP1 domain was plotted using custom scripts. Distance between the centroids of protein and the peptide was computed using snapshots taken at an interval of 0.5 ns for the entire simulation time. EWMA (Exponentially Weighted Moving Average) was used to understand average behaviour. The abundance of intramolecular hydrogen bonds was also plotted across the triplicate MD runs using a custom script built on top of UCSF Chimera.

4 RESULTS AND FINDINGS

4.1 OBTAINING THE COMPLEX FROM PROTEIN DATA BANK AND PRE-PROCESSING

The SWISS MODEL could not model specific amino acid sequences and were eliminated from the final model. This is summarised in Table 1.

<i>Chain ID</i>	<i>Eliminated residue number</i>
<i>A</i>	1-34; 435-472
<i>B</i>	170-179

Table 1: Deleted residue number after homology modelling

This may not affect this study since we know from the literature that these regions are not involved in their interaction [8]. During the process of homology modelling, all the non-standard residues and small molecules were removed.

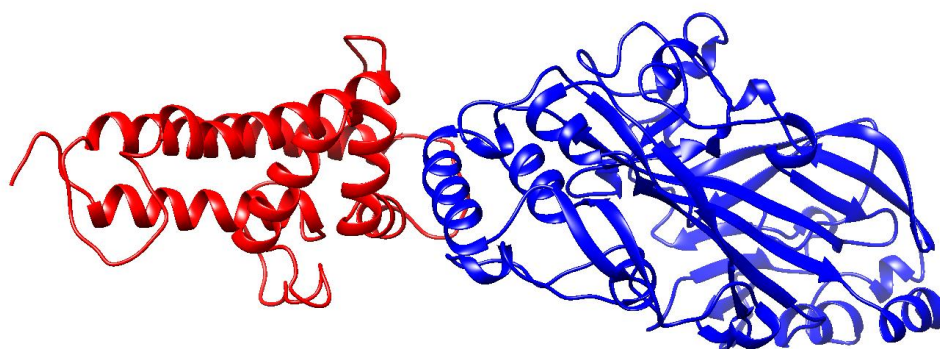


Figure 1: Interaction complex after homology modelling. The CIDRa domain is shown red and CD36 receptor protein in blue.

4.2 IDENTIFYING THE INTERACTING REGION

Using the approach mentioned in the Materials and Method section, a 10 amino acid sequence was identified from residue number 151 to 160 of chain A. The sequence is NQFVQMILNS. This is the wild type inhibitory sequence.

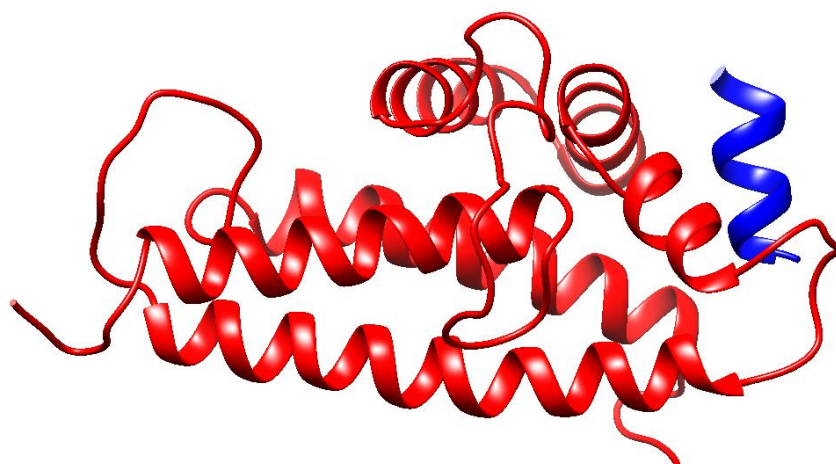


Figure 2: Identified wild type inhibitor. The inhibitor is shown in blue and the parasite protein in red

4.3 COMPUTATIONAL SATURATED MUTAGENESIS AND SCORING

After performing computational saturated mutagenesis on the identified wild type inhibitor of 10 amino acids, we got 200 mutants, including repeated sequences. This was scored using FoldX, and the result is summarised in Figure 3.



Figure 3: Heat map summarising the result of Computational Saturated Mutagenesis

Using the scores obtained a hybrid inhibitor was constructed. The sequence of the hybrid inhibitor is NKFWRWMWRM.

The details of the 3 shortlisted mutant inhibitor along with the hybrid and wild type inhibitor is summarised in Table 2.

<i>Inhibitor Number</i>	<i>Inhibitor type</i>	<i>Sequence</i>	<i>No. of amino acids</i>	<i>Interaction energy (kcal/mol)</i>
1	Hybrid	NKFWRWMWRM	10	-21.1723
2	Mutant	NQFVQMILNM	10	-18.8211
3	Mutant	NQFVQMILNF	10	-18.7332
4	Mutant	NQFVQMILNW	10	-18.4663
5	Wild	NQFVQMILNS	10	-16.5112

Table 2: Summary of potential inhibitors

4.4 MOLECULAR DYNAMICS SIMULATION OF THE INHIBITOR MODELS AND ITS ANALYSIS

One hybrid inhibitor and 3 mutant inhibitors were studied by performing MD simulations. All systems were found to be stable. A summary of various analysis for all inhibitor complexes is summarised in Table 3.

<i>Inhibitor Number</i>	<i>Inhibitor type</i>	<i>Sequence</i>	<i>Centroid distance (Å^0)</i>	<i>Number of Hydrogen bonds</i>
1	Hybrid	NKFWRWMWRM	22.29 ± 0.49	13
2	Mutant	NQFVQMILNM	21.86 ± 0.64	5
3	Mutant	NQFVQMILNF	22.13 ± 0.61	5
4	Mutant	NQFVQMILNW	22.41 ± 0.50	6
5	Wild	NQFVQMILNS	22.27*	5

Table 3: Summary of MD simulation data. (*: MD simulation was not performed; Centroid distance and hydrogen bond numbers were calculated based on the homology model from SWISS MODEL after identifying the interacting regions).

The RMSD plots had some minor fluctuations for all the inhibitors studied. Even though this might be an indication of protein unfolding, no significant unfolding was observed while visualising the trajectories. The observation can be attributed to the oscillatory motions of some loosely folded domains. Since the interacting complexes we studied was a part of the larger domain, these fluctuations may be neglected.

The plot showing the time evolution of the distance between the centroids is also fluctuating; in most cases, the EWMA shows a positive slope. This is an indication of the two interacting protein moving apart. But this was not observed while visualising the trajectory file. This could be due to the random movements of the loosely folded protein regions affecting the position of the calculated centre of mass.

By looking at the percentage abundance of hydrogen bonds across the runs for all the inhibitors, the hybrid peptide (inhibitor 1) ranks much higher. It has a total of 13 hydrogen

bond pairs compared to inhibitor 4 which ranks 2nd with only 6 hydrogen bond pairs. This was expected from its interaction energy and also from the way it was constructed.

The plots and tables for respective inhibitors are provided below within respective subsections.

4.4.1 Inhibitor 1: Hybrid

4.4.1.1 RMSD Plots

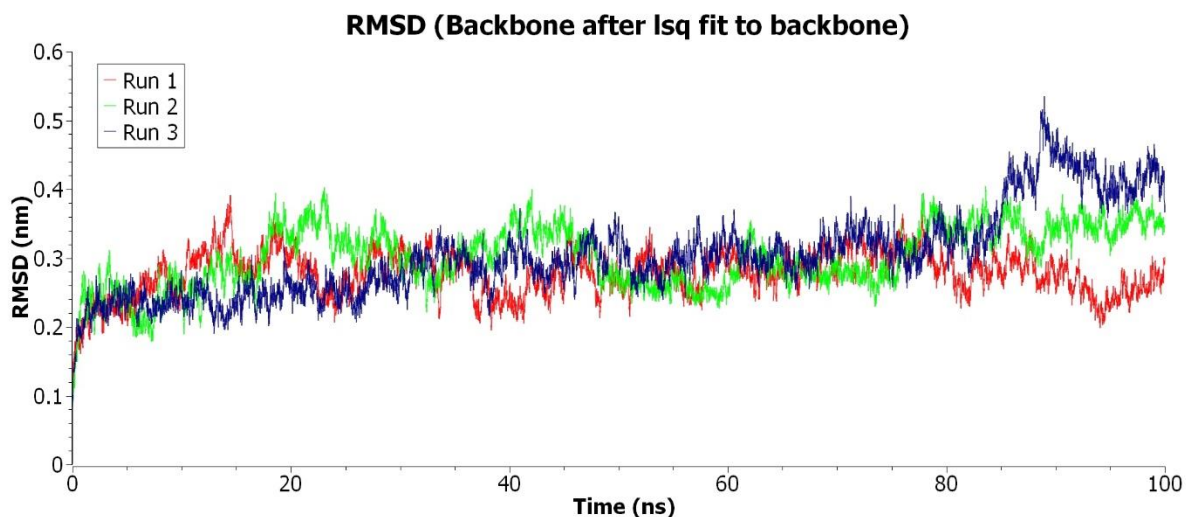


Figure 4: RMSD plot of inhibitor 1

4.4.1.2 Centroid Analysis

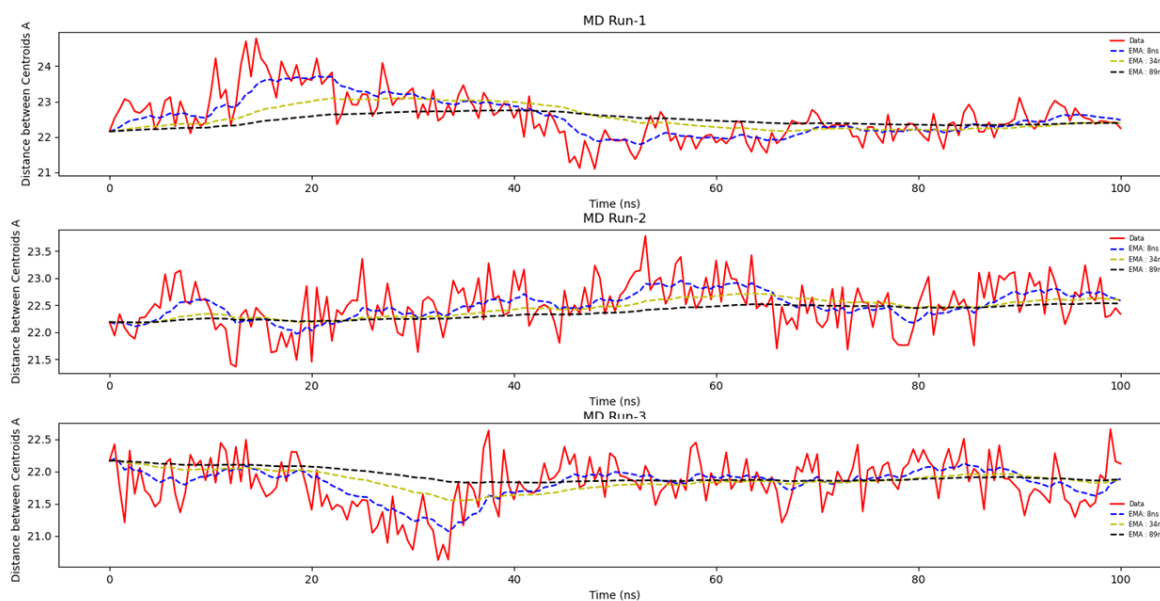


Figure 5: Centroid plot of inhibitor 1

4.4.1.3 Hydrogen bond analysis

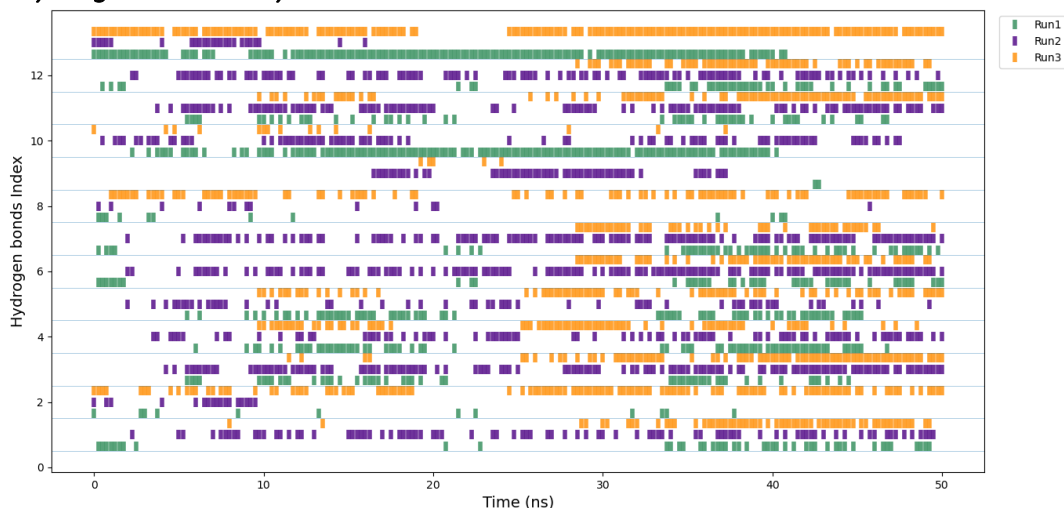


Figure 6: Hydrogen bond plot of inhibitor 1

Index	Hydrogen bond Acceptor-Donor	MD run 1 (%)	MD run 2 (%)	MD run 3 (%)
1	GLU:97.B.OE2 - ARG:159.A.NH2	22.39	43.28	30.35
2	ASP:75.B.OD1 - ASN:151.A.ND2	5.97	8.46	56.22
3	ASP:101.B.OD1 - ARG:155.A.NH1	24.88	61.19	37.81
4	ASP:101.B.OD2 - ARG:155.A.NH1	32.84	41.29	35.82
5	ASP:101.B.OD1 - ARG:155.ANH22	33.83	27.86	37.31
6	GLU:97.B.OE1 - ARG:159.A.NH2	21.89	63.18	28.86
7	GLU:97.B.OE2 - ARG:159.ANH1	23.88	60.20	22.39
8	ASP:75.B.OD2 - ASN:151.A.ND2	5.97	6.47	45.77
9	ASP:75.B.OD1 - LYS:152.A.N	1.00	26.37	2.49
10	ASP:75.B.O - ASN:151.A.ND2	63.68	41.29	7.46
11	ASP:101.B.OD2 - ARG:155.A.NH2	23.88	53.73	40.80
12	GLU:97.B.OE1 - ARG:159.A.NH1	22.39	52.24	29.85
13	GLN:73.B.OE1 - ASN:151.A.ND2	72.14	11.94	83.08

Table 4: Abundance of hydrogen bond pairs of inhibitor 1

4.4.2 Inhibitor 2: Mutant

4.4.2.1 RMSD Plots

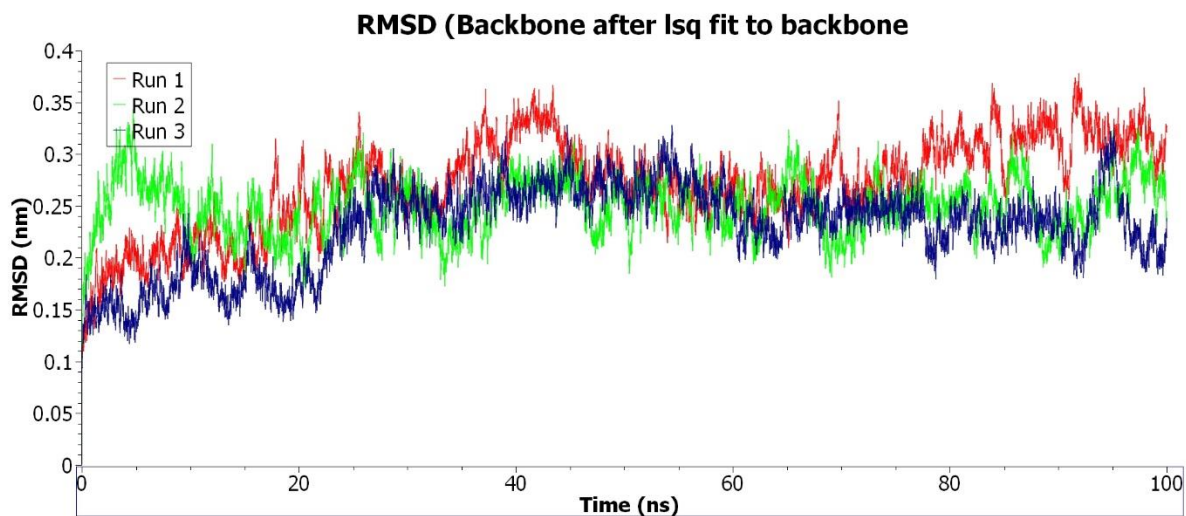


Figure 7: RMSD plot of inhibitor 2

4.4.2.2 Centroid Analysis

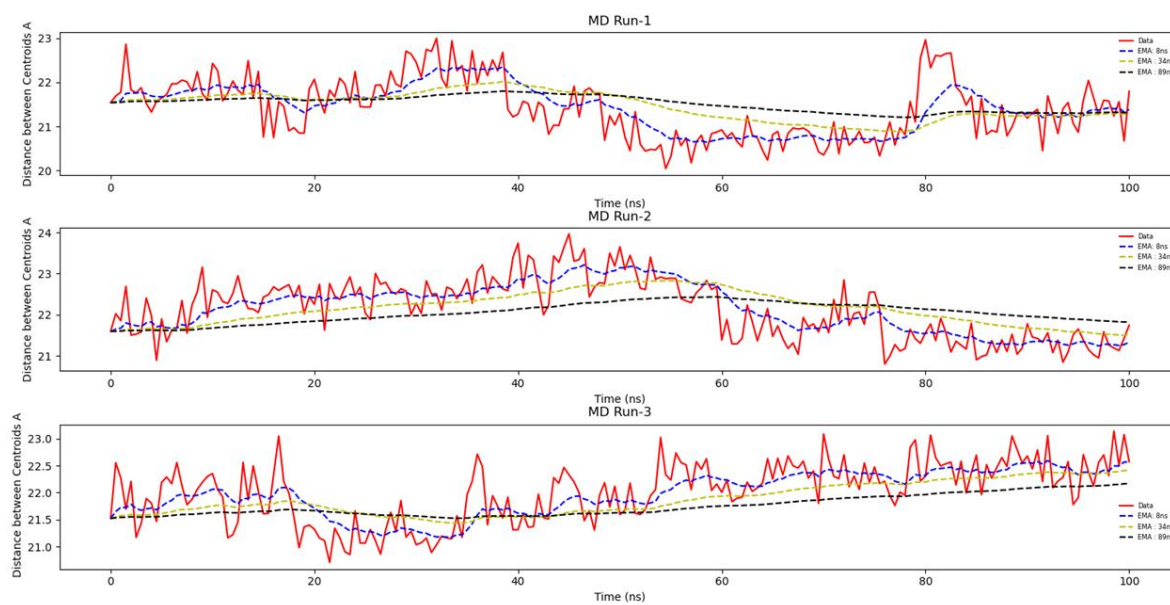


Figure 8: Centroid plot of inhibitor 2

4.4.2.3 Hydrogen bond analysis

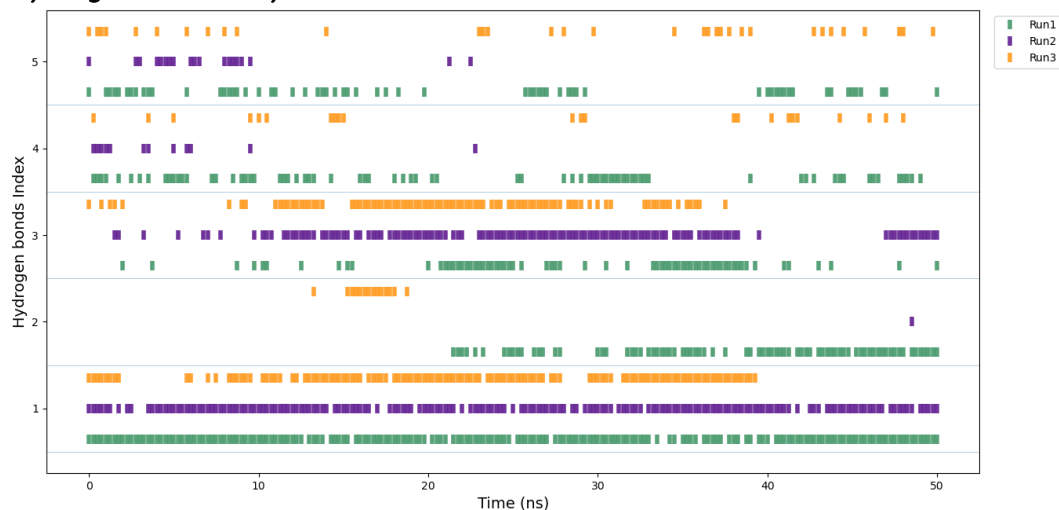


Figure 9: Hydrogen bond plot of inhibitor 2

Index	Hydrogen bond Acceptor-Donor	MD run 1 (%)	MD run 2 (%)	MD run 3 (%)
1	GLN:73.B.OE1 - ASN:151.A.ND2	92.04	88.06	59.70
2	GLN:152.A.OE1 - ASN:8.B.N	39.30	0.50	6.96
3	ASP:75.B.O - ASN:151.A.ND2	33.33	61.19	44.28
4	ASP:75.B.OD1 - ASN:151.A.ND2	36.32	5.97	11.44
5	ASP:75.B.OD2 - ASN:151.A.ND2	30.85	9.45	16.42

Table 5: Abundance of hydrogen bond pairs of inhibitor 2

4.4.3 Inhibitor 3: Mutant

4.4.3.1 RMSD Plots

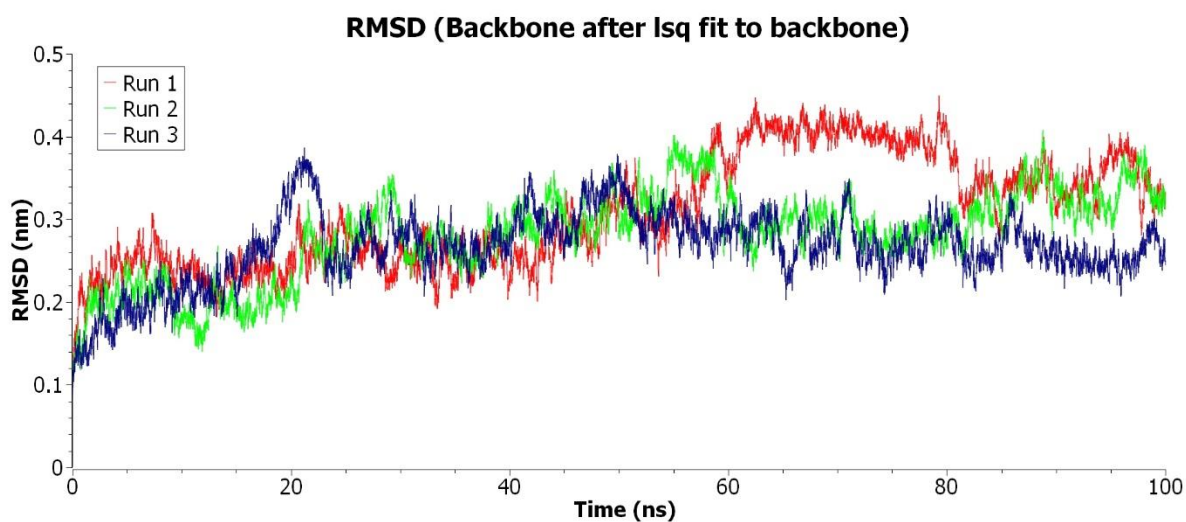


Figure 10: RMSD plot of inhibitor 3

4.4.3.2 Centroid Analysis

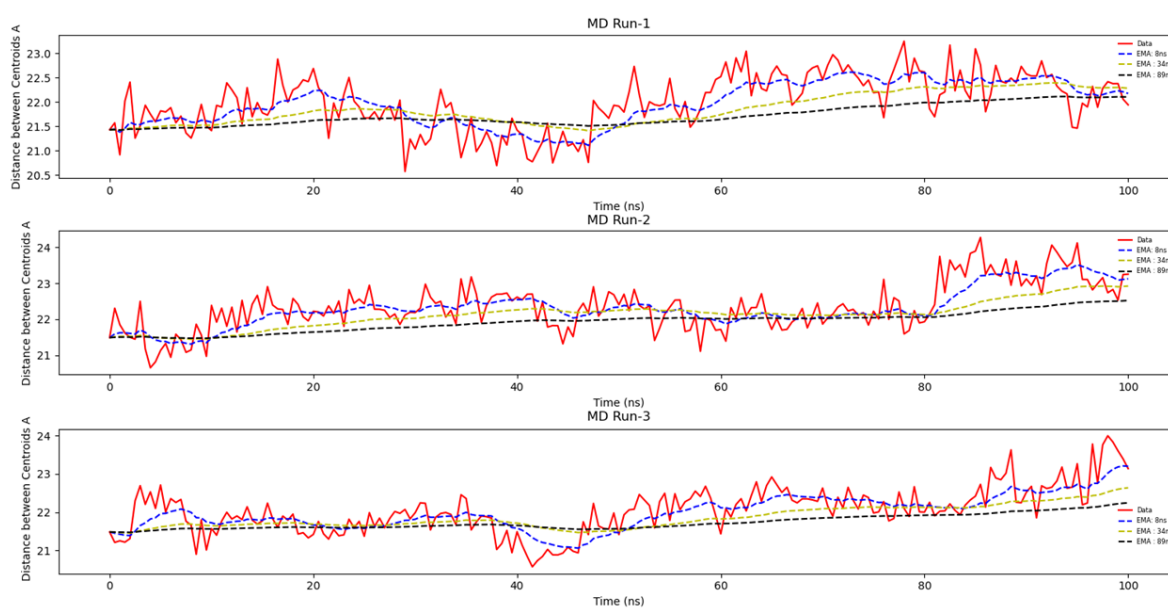


Figure 11: Centroid plot of inhibitor 3

4.4.3.3 Hydrogen bond analysis

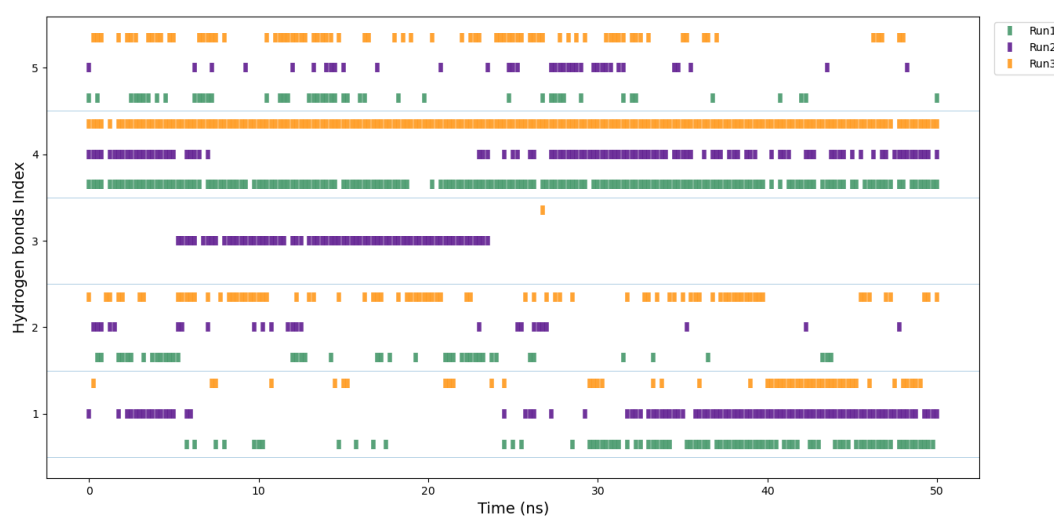


Figure 12: Hydrogen bond plot of inhibitor 3

Index	Hydrogen bond Acceptor-Donor	MD run 1 (%)	MD run 2 (%)	MD run 3 (%)
1	ASP:75.B.O - ASN:151.A.ND2	40.80	45.77	24.38
2	ASP:75.B.OD1 - ASN:151.A.ND2	20.90	12.44	39.80
3	GLN:152.A.OE1 - TRP:12.B.NE1	0	34.83	0.50
4	GLN:73.B.OE1 - ASN:151.A.ND2	90.05	50.75	98.51
5	ASP:75.B.OD2 - ASN:151.A.ND2	22.89	17.91	38.81

Table 6: Abundance of hydrogen bond pairs of inhibitor 3

4.4.4 Inhibitor 4: Mutant

4.4.4.1 RMSD Plots

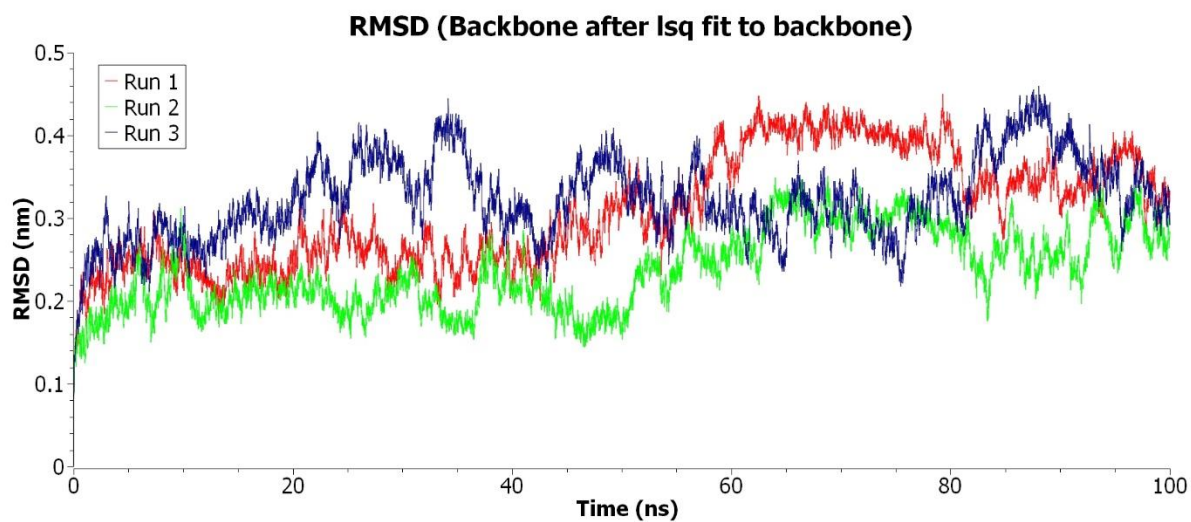


Figure 13: RMSD plot of inhibitor 4

4.4.4.2 Centroid Analysis

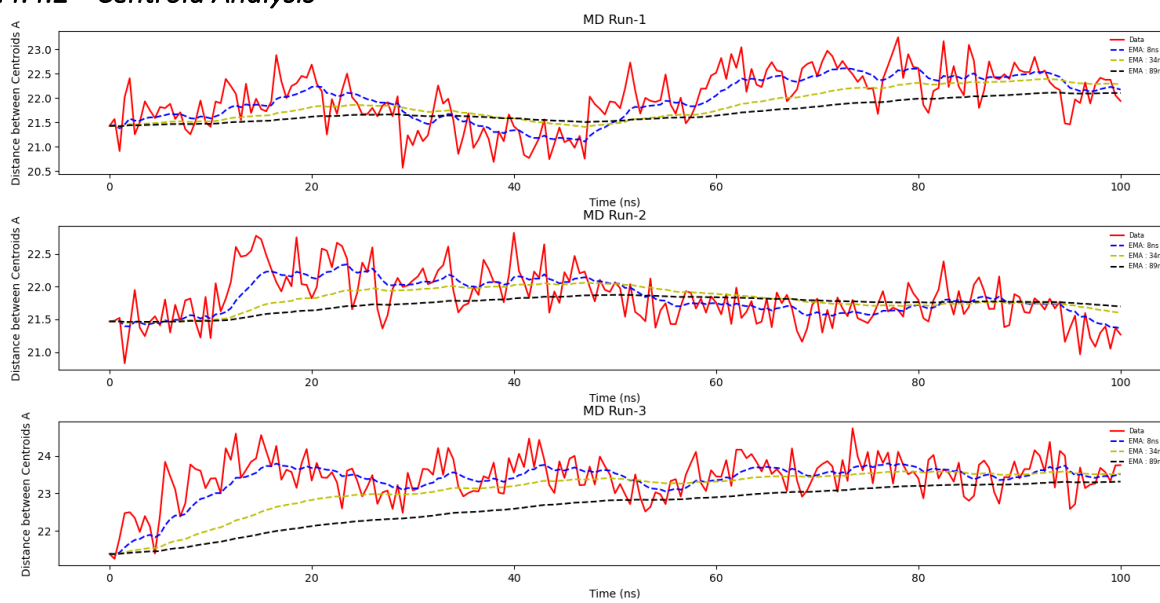


Figure 14: Centroid plot of inhibitor 4

4.4.4.3 Hydrogen bond analysis

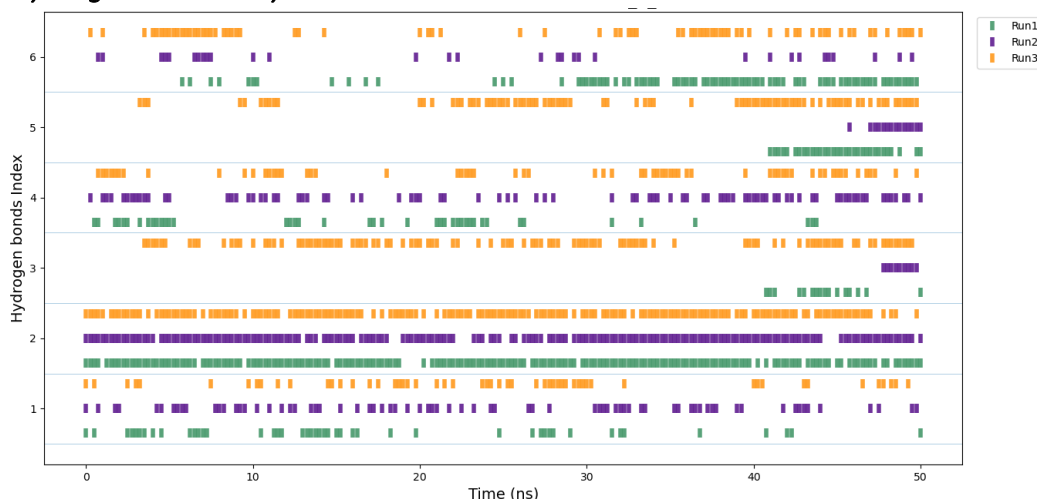


Figure 15: Hydrogen bond plot of inhibitor 4

Index	Hydrogen bond Acceptor-Donor	MD run 1 (%)	MD run 2 (%)	MD run 3 (%)
1	ASP:75.B.OD2 - ASN:151.A.ND2	22.89	36.82	27.36
2	GLN:73.B.OE1 - ASN:151.A.ND2	90.05	89.06	82.09
3	GLN:152.A.O - ASN:8.B.ND2	7.96	4.48	50.75
4	ASP:75.B.OD1 - ASN:151.A.ND2	20.90	42.29	30.85
5	GLN:152.A.OE1 - ASN:8.B.N	15.92	6.96	40.80
6	ASP:75.B.O - ASN:151.A.ND2	40.80	15.42	36.32

Table 7: Abundance of hydrogen bond pairs of inhibitor 4

5 DISCUSSION

Various computational techniques were used in designing peptide inhibitors against the interaction of the CIDRa domain of PfEMP1 and the CD36 receptor. In this study, I have studied how the 3 best-scored mutant and the hybrid inhibitor interact with the CIDRa domain. From the results obtained, the hybrid peptide (inhibitor 1) has the strongest interaction in terms of the number of intermolecular hydrogen bonds and the interaction energy values calculated by FoldX. But we should consider the fact that the hybrid peptide is the most mutated inhibitor with 8 out of the 10 amino acids mutated. Hence the immunogenicity of this inhibitor has to be assessed before proceeding further.

As the project aimed to graft these inhibitors to a cyclotide backbone, the number of amino acids may affect the stability of the cyclotide. If that may be the case, amino acids residues may be removed from both ends of the inhibitors provided it is not involved in the hydrogen bond pairs shown in the respective sections in the Results and findings section.

6 CONCLUSION

Four potential inhibitors against the interaction of CIDRa domain of PfEMP1 and CD36 receptor have been studied in this project using various computational tools. They can be used as a starting point for further studies for developing peptide-based inhibitors against falciparum malaria. The methods used in this study can be used for designing peptide inhibitors against other interactions against falciparum malaria as well as other diseases.

All the scripts used in this project can be found at our Github repository <https://github.com/igemsoftware2020/IISER-Pune-India>, and additional details can be found at our Team Wiki <https://2020.igem.org/Team:IISER-Pune-India>.

7 REFERENCES

- [1] Arkin, M. R., & Wells, J. A. (2004). Small-molecule inhibitors of protein-protein interactions: progressing towards the dream. *Nature Reviews Drug Discovery*, 4, 301–317. <https://doi.org/10.1038/nrd1343>
- [2] Berman, H. M. (2000). The Protein Data Bank. *Nucleic Acids Research*, 1, 235–242. <https://doi.org/10.1093/nar/28.1.235>
- [3] Bussi, G., Donadio, D., & Parrinello, M. (2007). Canonical sampling through velocity rescaling. *The Journal of Chemical Physics*, 1, 014101. <https://doi.org/10.1063/1.2408420>
- [4] Darden, T., York, D., & Pedersen, L. (1993). Particle mesh Ewald: AnN·log(N) method for Ewald sums in large systems. *The Journal of Chemical Physics*, 12, 10089–10092. <https://doi.org/10.1063/1.464397>
- [5] Gould, A., & Camarero, J. A. (2017). Cyclotides: Overview and Biotechnological Applications. *ChemBioChem*, 14, 1350–1363. <https://doi.org/10.1002/cbic.201700153>
- [6] Hamilton, W. L., Amato, R., van der Pluijm, R. W., Jacob, C. G., Quang, H. H., Thuy-Nhien, N. T., Hien, T. T., Hongvanthong, B., Chindavongsa, K., Mayxay, M., Huy, R., Leang, R., Huch, C., Dysoley, L., Amaratunga, C., Suon, S., Fairhurst, R. M., Tripura, R., Peto, T. J., ... Miotto, O. (2019). Evolution and expansion of multidrug-resistant malaria in southeast Asia: a genomic epidemiology study. *The Lancet Infectious Diseases*, 9, 943–951. [https://doi.org/10.1016/s1473-3099\(19\)30392-5](https://doi.org/10.1016/s1473-3099(19)30392-5)
- [7] Hess, B., Bekker, H., Berendsen, H. J. C., & Fraaije, J. G. E. M. (1997). LINCS: A linear constraint solver for molecular simulations. *Journal of Computational Chemistry*, 12, 1463–1472. [https://doi.org/10.1002/\(sici\)1096-987x\(199709\)18:12<1463::aid-jcc4>3.0.co;2-h](https://doi.org/10.1002/(sici)1096-987x(199709)18:12<1463::aid-jcc4>3.0.co;2-h)
- [8] Hsieh, F.-L., Turner, L., Bolla, J. R., Robinson, C. V., Lavstsen, T., & Higgins, M. K. (2016). The structural basis for CD36 binding by the malaria parasite. *Nature Communications*, 1. <https://doi.org/10.1038/ncomms12837>

- [9] Hughes, K. R., Biagini, G. A., & Craig, A. G. (2010). Continued cytoadherence of *Plasmodium falciparum* infected red blood cells after antimalarial treatment. *Molecular and Biochemical Parasitology*, *2*, 71–78. <https://doi.org/10.1016/j.molbiopara.2009.09.007>
- [10] Lindorff-Larsen, K., Piana, S., Palmo, K., Maragakis, P., Klepeis, J. L., Dror, R. O., & Shaw, D. E. (2010). Improved side-chain torsion potentials for the Amber ff99SB protein force field. *Proteins: Structure, Function, and Bioinformatics*, *8*, 1950–1958. <https://doi.org/10.1002/prot.22711>
- [11] Malaria. (n.d.-a). *Dangerous – MALARIA.com*. MALARIA.COM | Malaria Information, Research and News. Retrieved December 11, 2020, from <http://www.malaria.com/questions/dangerous>
- [12] *Malaria*. (n.d.-b). WHO | World Health Organization. Retrieved December 10, 2020, from <https://www.who.int/news-room/fact-sheets/detail/malaria>
- [13] Mark, P., & Nilsson, L. (2001). Structure and Dynamics of the TIP3P, SPC, and SPC/E Water Models at 298 K. *The Journal of Physical Chemistry A*, *43*, 9954–9960. <https://doi.org/10.1021/jp003020w>
- [14] Nov, Y. (2011). When Second Best Is Good Enough: Another Probabilistic Look at Saturation Mutagenesis. *Applied and Environmental Microbiology*, *1*, 258–262. <https://doi.org/10.1128/aem.06265-11>
- [15] Parrinello, M., & Rahman, A. (1981). Polymorphic transitions in single crystals: A new molecular dynamics method. *Journal of Applied Physics*, *12*, 7182–7190. <https://doi.org/10.1063/1.328693>
- [16] Pettersen, E. F., Goddard, T. D., Huang, C. C., Couch, G. S., Greenblatt, D. M., Meng, E. C., & Ferrin, T. E. (2004). UCSF Chimera?A visualisation system for exploratory research and analysis. *Journal of Computational Chemistry*, *13*, 1605–1612. <https://doi.org/10.1002/jcc.20084>
- [17] Schymkowitz, J., Borg, J., Stricher, F., Nys, R., Rousseau, F., & Serrano, L. (2005). The FoldX web server: an online force field. *Nucleic Acids Research, Web Server*, W382–W388. <https://doi.org/10.1093/nar/gki387>
- [18] Waterhouse, A., Bertoni, M., Bienert, S., Studer, G., Tauriello, G., Gumienny, R., Heer, F. T., de Beer, T. A. P., Rempfer, C., Bordoli, L., Lepore, R., & Schwede, T. (2018). SWISS-MODEL: homology modelling of protein structures and complexes. *Nucleic Acids Research*, *W1*, W296–W303. <https://doi.org/10.1093/nar/gky427>
- [19] Eswar, N., Webb, B., Marti-Renom, M. A., Madhusudhan, M. S., Eramian, D., Shen, M., Pieper, U., & Sali, A. (2006). Comparative Protein Structure Modeling Using Modeller. *Current Protocols in Bioinformatics*, *1*, 5.6.1-5.6.30. <https://doi.org/10.1002/0471250953.bi0506s15>
- [20] Schmidt, T. G., & Skerra, A. (2007). The Strep-tag system for one-step purification and high-affinity detection or capturing of proteins. *Nature Protocols*, *6*, 1528–1535. <https://doi.org/10.1038/nprot.2007.209>